Supporting Information

A Chiral Sodium Lanthanum Sulfate for Second-Order Nonlinear Optics and Proton Conduction

Hao Fu,[a,b] Xiaohui Zhang,[a] Peiyu Liu,[a] Bo Li,[c] Baolin Wu,[d] Ye Tao,[a] Qianshuang Lu,[a] Yingjie Li,[a] Jiaxi Huang,[a] Fangfang Zhang,[e] Tingchao He,[f] Zhi Chen,[a] Heng Wang,[g] Chenliang Su,[b] Hong-Ying Zang,[c] Xiujun Yu[a] and Xiaopeng Li[a,g,h]*

[a]College of Chemistry and Environmental Engineering, Shenzhen University, Shenzhen, Guangdong 518060, China

[b]Institute of Microscale Optoelectronics, Shenzhen University, Shenzhen, Guangdong 518060, China

[c]Key Laboratory of Polyoxometalate Science, Department of Chemistry, Northeast Normal University, Changchun, Jilin 130024, China

[d]Fundamental electrochemistry (IET-1), Institute of Energy Technologies, Forschungszentrum Jülich GmbH, Wilhelm-Johnen-Straße, Jülich 52425, Germany

[e]Research Center for Crystal Materials, Xinjiang Technical Institute of Physics and Chemistry, Chinese Academy of Sciences, Urumqi, Xinjiang 830011, China

[f]Key Laboratory of Optoelectronic Devices and Systems of Ministry of Education and Guangdong Province, College of Physics and Optoelectronic Engineering, Shenzhen University, Shenzhen, Guangdong 518060, China

[g]State Key Laboratory of Organometallic Chemistry, Shanghai Institute of Organic Chemistry, University of Chinese Academy of Sciences, Chinese Academy of Sciences, Shanghai 200032, China

[h]Shenzhen University General Hospital, Shenzhen University Clinical Medical Academy, Shenzhen University, Shenzhen, Guangdong 518055, China

*Corresponding Authors: xiujunyu@szu.edu.cn (X. Y.)

Table of Contents

1. Experimental Section

Materials and Instrumentation

Commercially available reagents were purchased from Macklin and used without further purification. Fourier transform infrared spectroscopy (FT-IR) data were collected on a Vertex70V Bruker FT-IR Spectrometer. UV/Vis-NIR spectra were recorded on a Shimadzu UV3600i spectrophotometer. Powder X-ray diffraction (PXRD) were measured on a Burker D8 diffractometer using Cu Kα radiation (λ = 1.54056Å) under ambient conditions. ICP-OES analyses were performed on a PerkinElmer Avio 200. Thermogravimetric analyses (TGA) were carried out on a Mettler Toledo TGA/SDTA 851e analyzer in air atmosphere with a heating rate of 10 ºC/min from 30 °C to 1000 °C.

Crystallographic Study

Single crystal X-ray diffraction data of $NaLa(SO_4)_2(H_2O)$ were collected on a Burker D8 Venture diffractometer with graphite-monochromatic Mo Kα radiation (λ = 0.7103 Å). Structure solutions and refinements were done with the OLEX2 software.[1]

Computational Methods

Crystal structure of $NaLa(SO_4)_2(H_2O)$ was used for theoretical calculations. Electronic structures and optical properties were calculated using a plane-wave basis set and pseudopotentials within density functional theory (DFT) implemented in the total energy code CASTEP.[2] For the exchange and correlation functional, we chose Perdew–Burke–Ernzerhof (PBE) in the generalized gradient approximation (GGA).[3] The interactions between the ionic cores and the electrons were described by the norm-conserving pseudopotential. Following valence-electron configurations were considered in the computation: Na $3s^12p^5$, La $5p^65d^16s^2$, S $3s^23p^5$, O $2s^22p^4$ and H $1s^1$. The numbers of plane waves included in the basis sets were determined by a kinetic-energy cutoff of 800 eV. Monkhorst–Pack k-point sampling of 4 × 4 × 2 was used to perform

numerical integration of the Brillouin zone for $NaLa(SO_4)_2(H_2O)$. The Fermi level was set to zero as the energy reference.

Synthesis of $NaLa(SO_4)_2(H_2O)$

The compound $NaLa(SO_4)_2(H_2O)$ was synthesized through a complementary strategy involving the combination of Na^+ and La^{3+}. Specifically, lanthanum sulfate (0.283 g, 0.5 mmol) and sodium sulfate (0.426 g, 3.0 mmol), were mixed at room temperature, and then H_2O (5 ml) was added. The resultant solution was heated at 200 °C for 3 days. After cooling to room temperature, colourless crystals of $NaLa(SO_4)_2(H_2O)$ were obtained. Yield: 120 mg (64%, based on lanthanum sulfate). ICP-OES Anal. Calcd for $NaLa(SO_4)_2(H_2O)$: La, 37.34; Na, 6.18. Found: La, 36.29; Na, 6.35. Notably, this synthetic protocol demonstrates robustness across a wide range of temperatures (120-200 °C), concentrations and pH levels.

NLO Performance Measurements

NLO properties of $NaLa(SO_4)_2(H_2O)$ were examined with a home-built scanning microscope with a femtosecond pump in reflection geometry, with the incidence and detection angles both at 45° (Fig. S7).[4] Linearly polarized pump was tuned with the λ/2 plate. Second-order NLO susceptibility of $NaLa(SO_4)_2(H_2O)$ was determined by using a Y-cut quartz as the reference. The effective second-order NLO coefficient, d_{eff}, of $NaLa(SO_4)_2(H_2O)$ was determined using a previous method.[5]

Proton Conductivity Measurements

Proton conductivity of $NaLa(SO_4)_2(H_2O)$ was measured using an impedance/ gain-phase analyzer (Solartron S1 1260) with a quasi-four-probe method over a frequency range from 1 Hz to 1 MHz within the input voltage of 100 mV. The measurements were operated at 30 °C with different relative humidity (50-98%) and under 98% relative humidity with various temperatures (30-85 °C). The impedances at each temperature were tested after equilibration for 30 min. Proton conductivities were calculated using our previous methods.[6,7]

2. Supporting Figures and Tables

Table S1 Crystallographic data of $NaLa(SO_4)_2(H_2O)$.

Compound	$NaLa(SO_4)_2(H_2O)$
Chemical Formula	$H_2LaNaO_9S_2$
Formula Mass	372.04
Crystal System	trigonal
a/Å	7.060(4)
b/Å	7.060(4)
c/Å	12.953(8)
α/°	90
β/°	90
γ/°	120
Volume/ Å^3	559.1(7)
ρ_{calc}g/cm^3	3.315
μ/mm^{-1}	6.371
Temperature/K	293.0
Space Group	$P3_221$
Z	3
No. of Reflections Measured	8223
No. of Independent Reflections	725
Rint	0.0912
Final R_1 Values ($I > 2\sigma(I)$)	0.0254
Final wR_2 Values ($I > 2\sigma(I)$)	0.0505
Goodness of Fit on F^2	1.092
Flack parameter	0.00(4)
CCDC Number	2351005

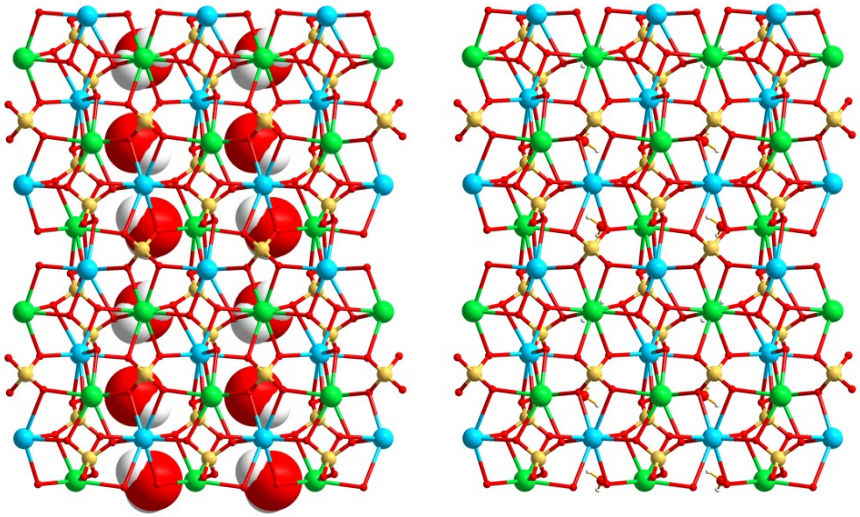

Fig. S1 View of $NaLa(SO_4)_2(H_2O)$ framework along the *a* or *b* axis.

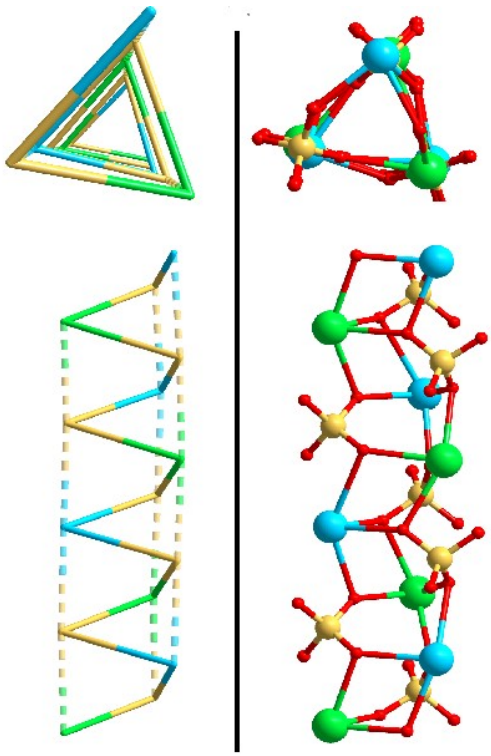

Fig. S2 1D triangular prism $[NaLa(SO_4)_2]_\infty$ and simplified topology of spiral chain of -La-S-Na-S-.

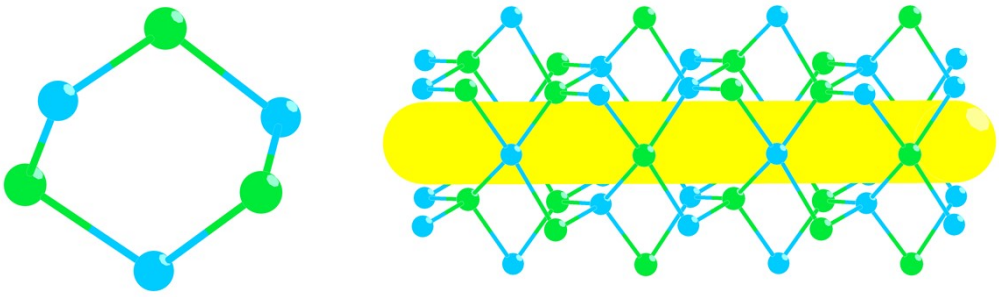

Fig. S3 Simplified topology of $\{Na_3La_3\}$ hexagonal ring (with sulfate units omitted) of the nanotube in $NaLa(SO_4)_2(H_2O)$.

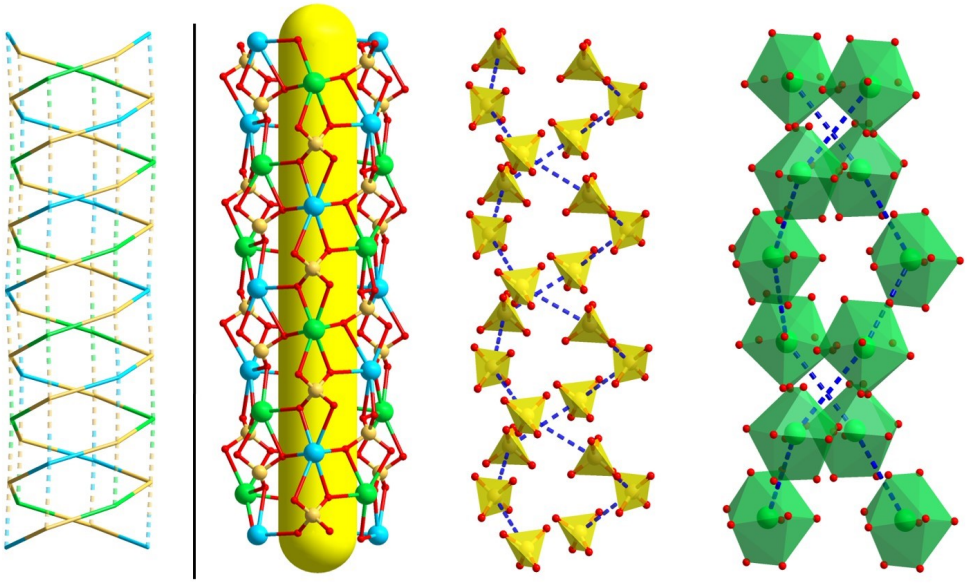

Fig. S4 Double helix of -La-S-Na-S- on the inner wall of the nanotube and simplified topology.

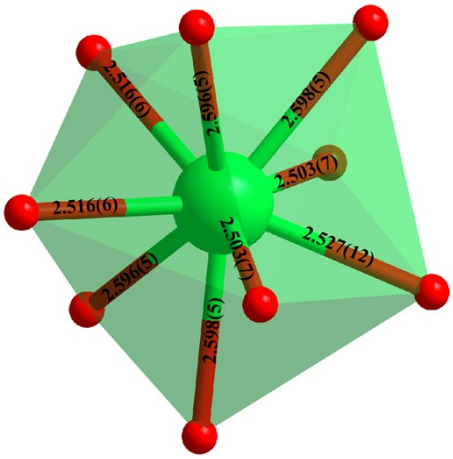

Fig. S5 $[LaO_9]$ polyhedron of $NaLa(SO_4)_2(H_2O)$ with bond distances.

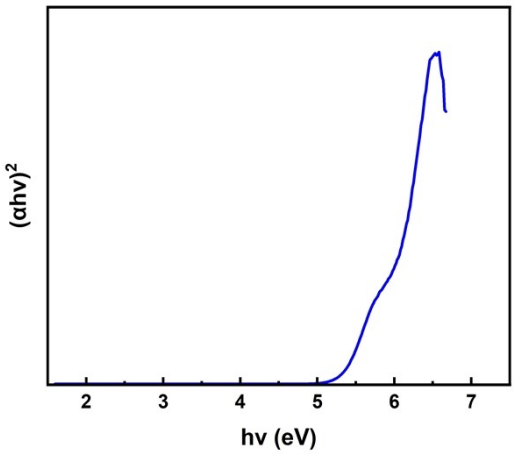

Fig. S6 Tauc plot of $NaLa(SO_4)_2(H_2O)$.

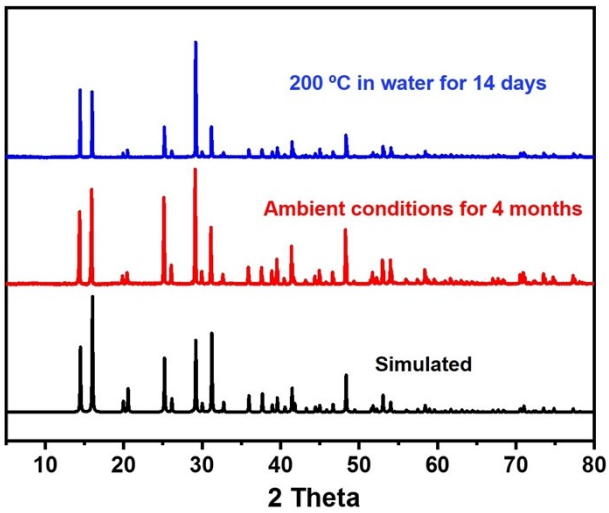

Fig. S7 PXRD patterns of $NaLa(SO_4)_2(H_2O)$ treated under different conditions.

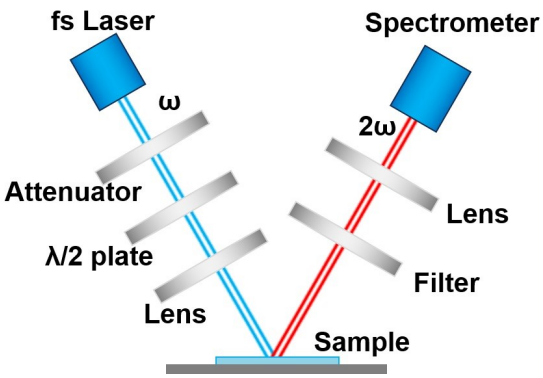

Fig. S8 Setup for measuring the NLO properties of $NaLa(SO_4)_2(H_2O)$.

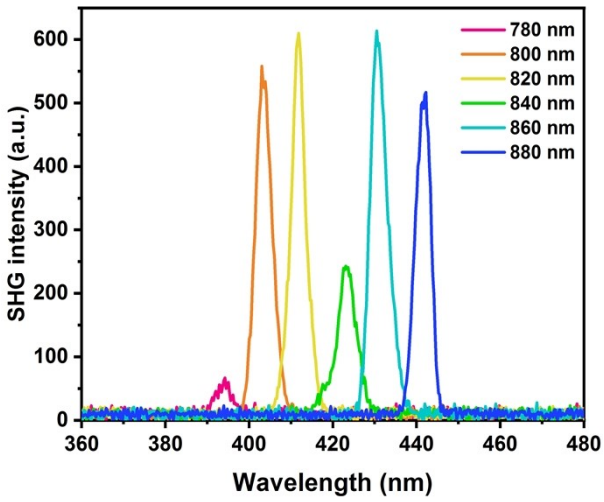

Fig. S9 SHG intensity of $NaLa(SO_4)_2(H_2O)$ crystal pumped at various wavelengths.

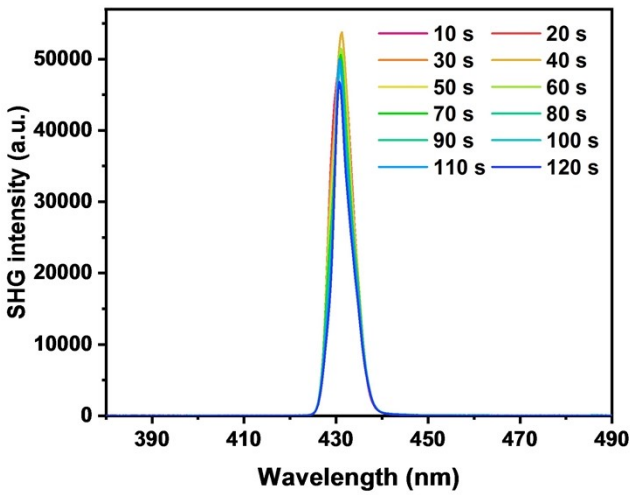

Fig. S10 SHG intensity of $NaLa(SO_4)_2(H_2O)$ crystal pumped at 860 nm for different time intervals with a excitation power of 150 mW.

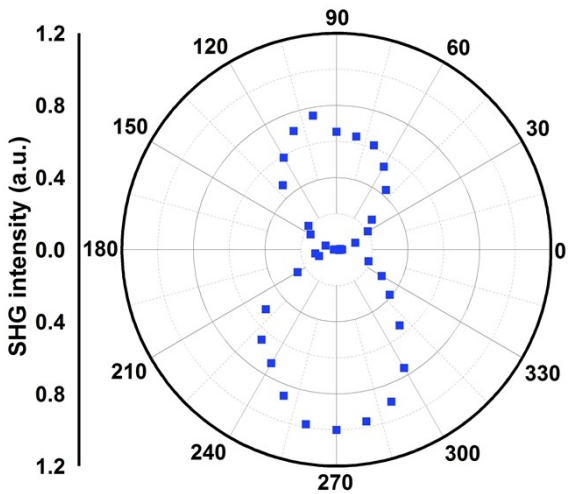

Fig. S11 Polar SHG intensity plots of $NaLa(SO_4)_2(H_2O)$ crystal as a function of the rotation angle of the linear polarizer.

Table S2 Fractional atomic coordinates ($\times 10^4$) and equivalent isotropic displacement parameters ($Å^2 \times 10^3$) for $NaLa(SO_4)_2(H_2O)$.

Atom	*x*	*y*	*z*	U(eq)
La01	0	-4325.8(10)	3333	11.01(18)
S002	5600(3)	128(3)	4199.5(11)	11.5(4)
Na03	4697(7)	4697(7)	5000	23.2(10)
O004	3826(10)	-1178(12)	3476(4)	18.7(15)
O005	6099(9)	-1288(9)	4846(4)	18.0(13)
O006	4965(10)	1345(10)	4922(4)	17.4(14)
O007	7539(8)	1627(9)	3593(4)	18.2(14)
O008	0	-746(16)	3333	57(5)

Table S3 Anisotropic displacement parameters ($Å^2 \times 10^3$) for $NaLa(SO_4)_2(H_2O)$.

Atom	U_{11}	U_{22}	U_{33}	U_{23}	U_{13}	U_{12}
La01	9.9(4)	11.5(3)	11.1(3)	0.04(14)	0.1(3)	4.9(2)
S002	12.1(9)	10.1(10)	10.2(8)	-0.1(8)	-0.3(7)	3.9(7)
Na03	27(2)	27(2)	21(2)	-2.8(11)	2.8(11)	18(3)
O004	15(3)	17(4)	15(3)	1(3)	-4(2)	2(3)
O005	23(4)	16(3)	17(3)	5(2)	2(2)	11(3)
O006	23(4)	21(3)	13(3)	-1(2)	-1(2)	15(3)
O007	11(3)	18(3)	20(3)	3(2)	5(2)	3(2)
O008	37(9)	24(5)	115(11)	12(3)	24(7)	18(5)

Table S4 Bond lengths for $NaLa(SO_4)_2(H_2O)$[a].

Atom	Atom	Length/Å	Atom	Atom	Length/Å
La01	O004	2.503(7)	S002	O006	1.483(6)
La01	O004^{4}	2.503(7)	S002	O007	1.471(5)
La01	O005^{2}	2.598(5)	Na03	O004^{9}	2.530(5)
La01	O005^{1}	2.598(5)	Na03	O004^{10}	2.530(5)
La01	O006^{1}	2.596(5)	Na03	O005^{11}	2.499(7)
La01	O006^{2}	2.596(5)	Na03	O005^{12}	2.499(7)
La01	O007^{5}	2.516(6)	Na03	O006	2.469(6)
La01	O007^{6}	2.516(6)	Na03	O006^{13}	2.469(6)
La01	O008	2.527(12)	Na03	O007^{9}	2.868(6)
S002	O004	1.464(6)	Na03	O007^{10}	2.868(6)
S002	O005	1.476(5)			

[a]Symmetry codes for $NaLa(SO_4)_2(H_2O)$: (1) y, x-1, -z+1; (2) -y, x-y-1, z-1/3; (3) -y+1, x-y, z-1/3; (4) -x, -x+y, -z+2/3; (5) x-1, y-1, z; (6) -x+1, -x+y, -z+2/3; (7) -x+y+1, -x, z+1/3; (8) x+1, y+1, z; (9) -x+y+1, -x+1, z+1/3; (10) -x+1, -x+y+1, -z+2/3; (11) x, y+1, z; (12) y+1, x, -z+1; (13) y, x, -z+1.

Table S5 Bond angles for $NaLa(SO_4)_2(H_2O)$.

Atom	Atom	Atom	Angle/°	Atom	Atom	Atom	Angle/°
O004^{4}	La01	O004	139.3(3)	O008	La01	O005^{1}	73.12(12)
O004^{4}	La01	O005^{2}	71.48(17)	O008	La01	O005^{2}	73.12(12)
O004^{4}	La01	O005^{1}	96.63(18)	O008	La01	O006^{1}	112.07(13)
O004	La01	O005^{2}	96.63(18)	O008	La01	O006^{2}	112.07(13)
O004	La01	O005^{1}	71.48(17)	O004^{8}	Na03	O004^{10}	151.3(4)
O004	La01	O006^{2}	76.74(19)	O004^{10}	Na03	O007^{10}	51.67(17)
O004	La01	O006^{1}	119.41(18)	O004^{10}	Na03	O007^{8}	142.5(2)
O004^{4}	La01	O006^{2}	119.41(18)	O004^{8}	Na03	O007^{10}	142.5(2)
O004^{4}	La01	O006^{1}	76.74(19)	O004^{8}	Na03	O007^{8}	51.67(17)
O004^{4}	La01	O007^{5}	145.5(2)	O005^{11}	Na03	O004^{10}	72.7(2)
O004^{4}	La01	O007^{6}	74.1(2)	O005^{11}	Na03	O004^{8}	85.3(2)
O004	La01	O007^{6}	145.5(2)	O005^{12}	Na03	O004^{8}	72.7(2)
O004	La01	O007^{5}	74.1(2)	O005^{12}	Na03	O004^{10}	85.3(2)
O004^{4}	La01	O008	69.63(17)	O005^{11}	Na03	O005^{12}	80.2(3)
O004	La01	O008	69.63(17)	O005^{12}	Na03	O007^{10}	88.67(17)
O005^{1}	La01	O005^{2}	146.2(2)	O005^{11}	Na03	O007^{8}	88.67(17)
O006^{2}	La01	O005^{1}	143.46(17)	O005^{11}	Na03	O007^{10}	123.99(17)
O006^{1}	La01	O005^{1}	54.18(17)	O005^{12}	Na03	O007^{8}	123.99(17)
O006^{1}	La01	O005^{2}	143.46(17)	O006^{13}	Na03	O004^{10}	113.74(18)
O006^{2}	La01	O005^{2}	54.18(17)	O006^{13}	Na03	O004^{8}	79.4(2)
O006^{1}	La01	O006^{2}	135.9(3)	O006	Na03	O004^{8}	113.74(18)
O007^{5}	La01	O005^{1}	85.81(17)	O006	Na03	O004^{10}	79.4(2)
O007^{5}	La01	O005^{2}	122.14(17)	O006^{13}	Na03	O005^{12}	76.55(17)
O007^{6}	La01	O005^{1}	122.14(17)	O006	Na03	O005^{11}	76.55(17)
O007^{6}	La01	O005^{2}	85.81(17)	O006^{13}	Na03	O005^{11}	155.1(3)
O007^{5}	La01	O006^{1}	77.07(18)	O006	Na03	O005^{12}	155.1(3)
O007^{6}	La01	O006^{1}	68.28(17)	O006	Na03	O006^{13}	127.7(4)
O007^{6}	La01	O006^{2}	77.07(18)	O006	Na03	O007^{10}	96.9(2)
O007^{5}	La01	O006^{2}	68.28(17)	O006^{13}	Na03	O007^{10}	64.55(16)
O007^{5}	La01	O007^{6}	75.6(2)	O006	Na03	O007^{8}	64.55(16)
O007^{6}	La01	O008	142.22(12)	O006^{13}	Na03	O007^{8}	96.9(2)
O007^{5}	La01	O008	142.22(12)	O007^{10}	Na03	O007^{8}	139.0(3)

3. References

[1] O. V. Dolomanov, L. J. Bourhis, R. J. Gildea, J. A. K. Howard and H. Puschmann, OLEX2: a complete structure solution, refinement and analysis program, *J. Appl. Cryst.*, **2009**, *42*, 339-341.

[2] S. J. Clark, M. D. Segall, C. J. Pickard, P. J. Hasnip, M. I. J. Probert, K. Refson and M. C. Payne, First principles methods using CASTEP, *Z. Kristallogr.,* **2005**, *220*, 567-570.

[3] J. Lin, M.-H. Lee, Z.-P. Liu, C. Chen and C. J. Pickard, Mechanism for linear and nonlinear optical effects in β-BaB_2O_4 crystals, *Phy. Rev. B*, **1999**, *60*, 13380-13389.

[4] Z. Guo, J. Li, J. Liang, C. Wang, X. Zhu and T. He, Regulating optical activity and anisotropic second-harmonic generation in zero-dimensional hybrid copper halides, *Nano Lett.,* **2022**, *22*, 846-852.

[5] P. Cheng, X. Jia, S. Chai, G. Li, M. Xin, J. Guan, X. Han, W. Han, S. Zeng, Y. Zheng, J. Xu and X.-H. Bu, Boosted second harmonic generation of a chiral hybrid lead halide resonant to charge transfer exciton from metal halide octahedra to ligand, *Angew. Chem., Int. Ed.,* **2024**, *63*, e202400644.

[6] B. Li, Y.-X. Meng, Q.-Q. Liu, X.-Y. Chen, X. Liu and H.-Y. Zang, The assembly of $[Mo_2O_2S_2]^{2+}$ based on polydentate phosphonate templates and their proton conductivity, *Chem. Commun.,* **2023**, *59*, 13446-13449.

[7] W.-B. Ren, S. Sun, Z. Gao, B. Li, X. Chen, Q. Liu and H.-Y. Zang, Synthesis of phosphovanadate-based porous inorganic frameworks with high proton conductivity, *Inorg. Chem.,* **2023**, *62*, 20506-20512.